Split-quaternions for perceptual white balance

Michel Berthier, Nicoletta Prencipe, Edoardo Provenzi

Split-quaternions for perceptual white balance

Michel Berthier*[1], Nicoletta Prencipe†[2] and Edoardo Provenzi‡[3]

[1]Laboratoire MIA, Bâtiment Pascal, Pôle Sciences et Technologies, Université de La Rochelle, 23, Avenue A. Einstein, BP 33060, 17031 La Rochelle Cedex, France
[2]Center for Ubiquitous Computing, Faculty of Information Technology and, Electrical Engineering, University of Oulu, Oulu, Finland
[3]Université de Bordeaux, CNRS, Bordeaux INP, IMB, UMR 5251, F-33400, 351 Cours de la Libération, Talence, France

Abstract

We propose a perceptual chromatic adaptation transform for white balance that makes use of split-quaternions. The novelty of the present work, which is motivated by a recently developed quantum-like model of color perception, consists at stressing the link between the algebraic structures appearing in this model and a certain sub-algebra of the split-quaternions. We show the potentiality of this approach for color image processing applications by proposing a chromatic adaptation transform, implemented via an appropriate use of the split-quaternion multiplication. Moreover, quantitative comparisons with the widely used state-of-the art von Kries chromatic adaptation transform are provided.

1 Introduction

The main objective of this work is to describe a new white balance algorithm that is implemented by means of split-quaternions. The peculiarity of this algorithm is the fact that it is designed to fit coherently with a recently developed mathematical model of color perception [9, 7]. This model provides an alternative to the CIE (Commission Internationale de l'Éclairage) description of colors by means of three coordinates in a colorimetric space, e.g. RGB, HSV, CIELab and so on. It also emphasizes the fact that a perceived color should be described as the result of a (perceptual) measurement procedure. The measurement equation, that is the cornerstone of the proposed algorithm, uses tools from quantum information and expresses the result of a so-called Lüders operation.

A complete mathematical description of this new paradigm about color perception is out of the scope of this work. For the sake of self-consistency, the essential concepts of this model will be recalled in section 2, the reader interested in more details can consult the following papers [9, 7, 4, 6, 8, 5]. We deem worthwhile to mention that this model permits to: intrinsically reconcile trichromacy with Hering's opponency [4, 6]; formalize Newton's chromatic disk [4]; single out the Hilbert-Klein hyperbolic metric as a natural perceptual chromatic distance [5]; solve the long-lasting problem of bounding the infinite perceptual color cone to a convex finite-volume solid of perceived colors [4, 9]; predict uncertainty relations for chromatic opposition [8] and give coherent mathematical definitions of perceived color perceptual attributes [7].

As we will underline with more detail in section 2, the color measurement equation takes place in the algebra $\mathcal{H}(2,\mathbb{R})$ of 2×2 symmetric matrices with real entries. To obtain a meaningful

*michel.berthier@univ-lr.fr
†nicoletta.prencipe@oulu.fi
‡edoardo.provenzi@math.u-bordeaux.fr

description of the measurement process, this algebra should not be considered as the associative, non-commutative algebra w.r.t. the matrix product, but rather as a non-associative, commutative algebra w.r.t. the product given by the symmetrized matrix product. Such a non-associative, commutative algebra is called a Jordan algebra, see e.g. [2] for more details.

As we will see in the following, three distinct incarnations of a certain suitable Jordan algebra $\mathcal{A}$ give rise to three different perspectives on color measurements:

1. $\mathcal{A}$ viewed as $\mathcal{H}(2,\mathbb{R})$, gives a quantum information point of view, where color measurements are expressed via the so-called Lüders operations;

2. $\mathcal{A}$ viewed as the direct sum $\mathbb{R}\oplus\mathbb{R}^2$ provides a geometric and relativistic interpretation, where color measurements are expressed via normalized Lorentz boosts in the 3-dimensional Minkowski space-time;

3. $\mathcal{A}$ viewed as a sub-algebra $\mathbb{S}_0$ of the split-quaternion algebra $\mathbb{S}$ brings a purely algebraic point of view, in which simple algebraic operations on split-quaternions allow us to encode color measurements.

The three representations of $\mathcal{A}$ are linked by explicit Jordan algebra isomorphisms, which allow us to pass from one to another and to obtain a simple formula for the measurement process by means of split-quaternions. It is precisely this formula that can be efficiently implemented in the white balance algorithm. Although understanding all these mathematical arguments is not necessary in practice to perform experiments, and maybe readers more interested in the computational aspects would prefer to skip them and to focus on Sec. 3 and 4, we deem important to underline that the proposed algorithm relies on a rigorous mathematical modeling of color perception.

The outline of the paper is the following: in Sec. 2 we start by introducing the basic definitions and notations necessary to formulate the measurement equation that defines a color perceived by an observer from a visual scene. We also explain how color measurements can be interpreted geometrically by means of Lorentz boosts. Sec. 3 is devoted to the split-quaternion point of view. After recalling some preliminary notions, we show how to encode the measurement equation by a so-called 'sandwich formula'. We also make explicit the geometric operations in $\mathbb{R}^4$ corresponding to this last formula to explain the difference with the usual sandwich formula involving the split-quaternion conjugacy. Experiments with the white balance algorithm are presented in Sec. 4. The practical implementation is detailed through appropriate approximations of a suitable subset of $\mathbb{S}_0$ used in the measurement equation. Comparisons with the well-known von Kries algorithm are also presented.

2 Color perception and color measurements

As said in the introduction, the proposed algorithm for white balance relies on a measurement equation that describes, from a quantum information point of view, the color perceived by an observer from a visual scene. The purpose of this section is to introduce the basic definitions and notations that permit to describe this equation. For additional information the interested reader may consult the references mentioned in the introduction.

2.1 Color measurements and quantum information

$\mathcal{H}(2,\mathbb{R})$, endowed with the Jordan product $A\circ B=(AB+BA)/2$, is a commutative, but not associative, Jordan algebra with domain of positivity $\overline{\mathcal{H}^+}(2,\mathbb{R})$, given by the set of real positive semi-definite 2×2 matrices. As usual in quantum information, mesurements are described by the duality between states and effects. In the context of color perception, the state space is that of a rebit, the real analog of a qubit, with the complex vector space $\mathbb{C}^2$ replaced by the real vector space $\mathbb{R}^2$. In [9, 7] it is explained why this quantum structure, that emerges from the sole axiomatic

approach, is perfectly adapted to translate mathematically Hering's color opponency. A so-called chromatic state $\mathbf{s}$ is represented by a density matrix $\rho_{\mathbf{s}}$:

$$\rho_{\mathbf{s}} = \frac{1}{2}\begin{pmatrix} 1+s_1 & s_2 \\ s_2 & 1-s_1 \end{pmatrix}, \tag{1}$$

with $1 - s_1^2 - s_2^2 \geq 0$, or equivalently by a chromatic vector $\mathbf{v_s} = (s_1, s_2)$, with $||\mathbf{v_s}|| \leq 1$. An effect $\mathbf{e}$ is represented by a matrix $\eta_{\mathbf{e}}$:

$$\eta_{\mathbf{e}} = \begin{pmatrix} e_0+e_1 & e_2 \\ e_2 & e_0-e_1 \end{pmatrix} = e_0\begin{pmatrix} 1+e_1/e_0 & e_2/e_0 \\ e_2/e_0 & 1-e_1/e_0 \end{pmatrix}, \tag{2}$$

such that $\mathbf{0} \leq \eta_{\mathbf{e}} \leq Id_2$, or equivalently by a chromatic vector $\mathbf{v_e} = (e_1/e_0, e_2/e_0)$ with $||\mathbf{v_e}|| \leq 1$ and $0 \leq e_0 \leq 1$. Given an effect $\mathbf{e}$, associated to a human observer, and a chromatic state $\mathbf{s}$, associated to the preparation of a visual scene, we have that the color perceived, or measured, by $\mathbf{e}$ from $\mathbf{s}$ is encoded in the outcome of the so-called Lüders operation parametrized by $\mathbf{e}$ and acting on $\mathbf{s}$, explicitly [10]:

$$\psi_{\mathbf{e}}(\mathbf{s}) = \eta_{\mathbf{e}}^{1/2}\rho_{\mathbf{s}}\eta_{\mathbf{e}}^{1/2}. \tag{3}$$

This last formula is the main topic of interest of this work. It is shown in [7] how it naturally permits to derive a coherent system of mathematical definitions of the CIE perceptual attributes, such as lightness, brightness, saturation and hue, using quantum information tools such as relative entropy.

2.2 Color measurements and Lorentz boosts

The commutative Jordan product of the so-called spin factor $\mathbb{R}\oplus\mathbb{R}^2$ is given by $(\alpha, \mathbf{v}) \circ (\beta, \mathbf{w}) = (\alpha\beta + \langle \mathbf{v}, \mathbf{w}\rangle, \alpha\mathbf{w} + \beta\mathbf{v})$ with $\alpha, \beta \in \mathbb{R}$, $\mathbf{v}, \mathbf{w} \in \mathbb{R}^2$. The domain of positivity of $\mathbb{R}\oplus\mathbb{R}^2$ is $\overline{\mathcal{L}^+} = \{(\alpha, \mathbf{v})^t \in \mathbb{R}\oplus\mathbb{R}^2,\ \alpha \geq 0,\ \alpha^2 - \|\mathbf{v}\|^2 \geq 0\}$, which is the closure of the future lightcone in the 3-dimensional Minkowski space-time $\mathcal{M}$. The two Jordan algebras $\mathcal{H}(2,\mathbb{R})$ and $\mathbb{R}\oplus\mathbb{R}^2$ are isomorphic, as Jordan algebras, via the following map:

$$\begin{array}{rccc} \chi: & \mathcal{H}(2,\mathbb{R}) & \xrightarrow{\sim} & \mathbb{R}\oplus\mathbb{R}^2 \\ & \begin{pmatrix} \alpha+v_1 & v_2 \\ v_2 & \alpha-v_1 \end{pmatrix} & \longmapsto & \begin{pmatrix} \alpha \\ v_1 \\ v_2 \end{pmatrix}. \end{array} \tag{4}$$

Clearly $\chi(\overline{\mathcal{H}^+}(2,\mathbb{R})) = \overline{\mathcal{L}^+}$. Using the isomorphism χ, we can interpret eq. (3) of color measurements as the action of a geometric transformation on $\mathcal{M}$. Given a chromatic state $\mathbf{s}$ and an effect $\mathbf{e}$ parameterized by the vectors $\mathbf{v_s} = (s_1, s_2)$ and $\mathbf{v_e} = (e_1/e_0, e_2/e_0)$, respectively, it is shown in [9] that, whenever $||\mathbf{v_e}|| < 1$ we have

$$\chi(\psi_{\mathbf{e}}(\mathbf{s})) = \frac{e_0}{\gamma_{\mathbf{v_e}}} B(\mathbf{v_e})\frac{1}{2}\begin{pmatrix} 1 \\ \mathbf{v_s} \end{pmatrix} \tag{5}$$

where

$$\gamma_{\mathbf{v_e}} = \frac{1}{\sqrt{1-||\mathbf{v_e}||^2}} \tag{6}$$

and the matrix representation of $B(\mathbf{v_e})$ is given by

$$[B(\mathbf{v_e})] = \begin{pmatrix} \gamma_{\mathbf{v_e}} & \gamma_{\mathbf{v_e}}\mathbf{v_e}^t \\ \gamma_{\mathbf{v_e}}\mathbf{v_e} & \sigma_0 + \frac{\gamma_{\mathbf{v_e}}^2}{1+\gamma_{\mathbf{v_e}}}\mathbf{v_e}\mathbf{v_e}^t \end{pmatrix}, \tag{7}$$

which can be recognized to be the Lorentz boost of $\mathcal{M}$ parameterized by the vector $\mathbf{v_e}$.

According to Minkowski geometry, this boost leaves the future lightcone invariant. The right-hand side of eq. (5) is the vector of $\overline{\mathcal{L}^+}$ that represents the outcome of the measurement given

by eq. (3). Besides emphasizing the relativistic aspect of color perception, see also [9, 5], this geometric description is very useful to analyze transformations between perceived color and to design white balance algorithms, as it will be discussed in the sequel.

The isomorphism χ provides a bridge between the two different perspectives on color measurements given by quantum information and Minkowski geometry. We underline here that eq. (3) expresses precisely the way in which an observer, represented by an effect, perceives a color of a visual scene prepared for a measurement in a given state. This description is radically different from the usual CIE color description because it relies on the very act of perceiving, and the geometric transformation in eq. (5) corresponds actually to perceived color measurements.

3 Color measurements and split-quaternions

We describe now the last Jordan algebra $\mathbb{S}_0$ which is a sub-algebra of the split-quaternion algebra, and how to encode with simple algebraic equations the previous color measurement formulas by means of the so-called 'sandwich formulas'.

3.1 The algebra of split-quaternions

The non-commutative, associative algebra of split-quaternions $\mathbb{S}$ is generally introduced in a similar way as the usual algebra of Hamilton's quaternions $\mathbb{H}$, see e.g. [12, 13, 18] for more details. There are four basis elements, denoted by $1, i, j, k$, however, differently from classic quaternions[1], i and j are such that $i^2 = j^2 = 1$, furthermore $ij = -ji$. The element k is defined as $k = ij$, this implies that $k^2 = -1$. Moreover, the following multiplication rules hold: $kj = -jk = i$ and $ik = -ki = j$. Every split-quaternion q can be written as

$$q = q_0 + q_1 i + q_2 j + q_3 k, \tag{8}$$

with $q_i \in \mathbb{R}$, $i \in \{0, \dots, 3\}$. The real constant q_0 is called the scalar part of q, while $\mathbf{v}_q := q_1 i + q_2 j + q_3 k$ is its vector part. The multiplication of two generic split-quaternions $q, r \in \mathbb{S}$ can be easily computed by writing them in the form of eq. (8) and then using the multiplication rules described above, obtaining the following explicit expression:

$$\begin{aligned} qr = \quad & q_0 r_0 + q_1 r_1 + q_2 r_2 - q_3 r_3 + (q_0 r_1 + q_1 r_0 - q_2 r_3 + q_3 r_2) i \\ & + (q_0 r_2 + q_2 r_0 + q_1 r_3 - q_3 r_1) j + (q_0 r_3 + q_3 r_0 + q_1 r_2 - q_2 r_1) k. \end{aligned} \tag{9}$$

In the same way as in the usual quaternion algebra $\mathbb{H}$, the conjugate q^* of a split-quaternion q is obtained by changing the sign of its vector part. The squared norm of a split-quaternion is given by $N^2(q) = qq^* = q_0^2 - q_1^2 - q_2^2 + q_3^2$. Differently from $\mathbb{H}$, N^2 is not positive-definite and the split-quaternions are classified according to the sign of $N^2(q)$: if $N^2(q) < 0$, q is *space-like*; if $N^2(q) = 0$, q is *light-like* and if $N^2(q) > 0$, q is *time-like*.

We denote with $\mathbb{S}_s$, $\mathbb{S}_l$ and $\mathbb{S}_t$ the subsets of $\mathbb{S}$ containing space-like, light-like and time-like split quaternions, respectively. If $q \in \mathbb{S}_t$, then $\mathbf{v}_q$ can belong to both $\mathbb{S}_s$ and $\mathbb{S}_t$. However, if $q \in \mathbb{S}_s$, then $\mathbf{v}_q$ can only belong to $\mathbb{S}_s$. The first statement follows from the fact that, if $q \in \mathbb{S}_t$, then $q_0^2 + q_3^2 > q_1^2 + q_2^2$, so both the cases $q_1^2 + q_2^2 < q_3^2$ or $q_3^2 < q_1^2 + q_2^2$ are possible, implying $N^2(\mathbf{v}_q) = -q_1^2 - q_2^2 + q_3^2 > 0$ or $N^2(\mathbf{v}_q) = -q_1^2 - q_2^2 + q_3^2 < 0$, i.e. $\mathbf{v}_q \in \mathbb{S}_t$ or $\mathbf{v}_q \in \mathbb{S}_s$, respectively.

To verify the last statement, consider $q \in \mathbb{S}_s$, then $q_0^2 + q_3^2 < q_1^2 + q_2^2$, which implies $q_3^2 < q_1^2 + q_2^2$, thus $N^2(\mathbf{v}_q) = -q_1^2 - q_2^2 + q_3^2 < 0$ and so $\mathbf{v}_q \in \mathbb{S}_s$.

Contrary to $\mathbb{H}$, $\mathbb{S}$ is not a division ring. In fact, it is easy to show that light-like split-quaternions do not admit a multiplicative inverse. The non-commutative, associative algebra $\mathbb{S}$ is isomorphic to the algebra of 2×2 matrices with real entries via the following map

$$\begin{array}{rccc} \zeta : & \mathbb{S} & \xrightarrow{\sim} & \mathcal{M}(2, \mathbb{R}) \\ & q_0 + q_1 i + q_2 j + q_3 k & \longmapsto & \begin{pmatrix} q_0 + q_1 & q_2 + q_3 \\ q_2 - q_3 & q_0 - q_1 \end{pmatrix}. \end{array} \tag{10}$$

[1] In classic quaternions i and j are imaginary units, hence $i^2 = j^2 = -1$, while in the split-quaternions algebra they are roots of the unity.

The split-quaternion multiplication corresponds to the matrix multiplication via ζ, hence $\zeta(qr) = \zeta(q)\zeta(r)$, for all $q, r \in \mathbb{S}$.

3.2 The sub-algebra $\mathbb{S}_0$ of the split-quaternion algebra

Let us denote $\mathbb{S}_0$ the set of split-quaternions such that $q_3 = 0$, so every $q \in \mathbb{S}_0$ has the following form $q = q_0 + q_1 i + q_2 j$. $\mathbb{S}_0$ becomes a commutative but not associative Jordan algebra when it is equipped with the Jordan product $q \circ r = (qr + rq)/2$. The restriction of ζ to $\mathbb{S}_0$, still denoted with ζ for simplicity, induces the following isomorphism of Jordan algebras:

$$\begin{array}{rccc} \zeta: & \mathbb{S}_0 & \xrightarrow{\sim} & \mathcal{H}(2,\mathbb{R}) \\ & q_0 + q_1 i + q_2 j & \longmapsto & \begin{pmatrix} q_0 + q_1 & q_2 \\ q_2 & q_0 - q_1 \end{pmatrix}. \end{array} \tag{11}$$

As a consequence, if $\overline{\mathbb{S}_0^+}$ indicates the domain of positivity of $\mathbb{S}_0$, then $\zeta(\overline{\mathbb{S}_0^+}) = \overline{\mathcal{H}^+}(2,\mathbb{R})$. If σ_1 and σ_2 denote the Pauli matrices with real entries, i.e.

$$\sigma_1 = \begin{pmatrix} 1 & 0 \\ 0 & -1 \end{pmatrix}, \quad \sigma_2 = \begin{pmatrix} 0 & 1 \\ 1 & 0 \end{pmatrix} \tag{12}$$

then $\zeta^{-1}(\sigma_1) = i$, $\zeta^{-1}(\sigma_2) = j$. The real Pauli matrices play a fundamental role in the quantum interpretation of color perception since they encode Hering's opponent mechanism, see e.g. [4, 9].

The spin factor $\mathbb{R} \oplus \mathbb{R}^2$ is isomorphic, as a Jordan algebra, to the commutative and non-associative sub-algebra of the Clifford algebra $CL(2, Q)$, where Q is the positive definite quadratic form on $\mathbb{R}^2$, linearly generated by the unit 1 and a spin system of $CL(2, Q)$. Let us recall that the Clifford algebra $CL(2, Q)$ is the quotient of the tensor algebra

$$T(\mathbb{R}^2) = \mathbb{R} \oplus \mathbb{R}^2 \oplus (\mathbb{R}^2 \otimes \mathbb{R}^2) \oplus \cdots = \bigoplus_{i \geq 0} (\mathbb{R}^2)^{\otimes i} \tag{13}$$

by the two-sided ideal $\mathcal{I}(\mathbb{R}^2, Q)$ generated by the elements of the form $u \otimes u - Q(u)$, for u in $\mathbb{R}^2$. For further details the interested reader can consult e.g. [20].

Since $CL(2, Q)$ is isomorphic to $\mathbb{S}$, this means that the map

$$\begin{array}{rccc} \omega: & \mathbb{S}_0 & \xrightarrow{\sim} & \mathbb{R} \oplus \mathbb{R}^2 \\ & q_0 + q_1 i + q_2 j & \longmapsto & (q_0, q_1, q_2)^t, \end{array} \tag{14}$$

is an isomorphism of Jordan algebras.

This completes the description of the three perspectives on color measurements listed in the introduction. The following commutative diagram of isomorphisms gives a concise mathematical representation of the relations between these perspectives:

$$\begin{array}{ccc} \mathcal{H}(2,\mathbb{R}) & \xrightarrow{\quad\chi\quad} & \mathbb{R} \oplus \mathbb{R}^2 \\ & {\scriptstyle\zeta}\nwarrow \quad \nearrow{\scriptstyle\omega} & \\ & \mathbb{S}_0 & \end{array} \tag{15}$$

According to what has been discussed before, this means that transformations corresponding to perceived color measurements can be computed in the split-quaternion framework.

3.3 The sandwich formula for color measurements

Our aim here is to express the original measurement equation (3), which was written in the setting of the Jordan algebra $\mathcal{H}(2,\mathbb{R})$ and its geometric counterpart expressed by eq. (5), which exploited the isomorphism with the spin-factor $\mathbb{R} \oplus \mathbb{R}^2$, in terms of split-quaternions by making use of the Jordan algebra $\mathbb{S}_0$.

To do so, we use the isomorphism ζ defined in eq. (11) and the definitions (1) and (2) of density and effect matrix, respectively. It is clear that, if we define the two split quaternions $p_{\mathbf{e}}, q_{\mathbf{s}} \in \overline{\mathbb{S}_0^+}$ as follows

$$p_{\mathbf{e}} = e_0 + e_1 i + e_2 j, \quad q_{\mathbf{s}} = (1 + s_1 i + s_2 j)/2, \tag{16}$$

then

$$\chi(\psi_{\mathbf{e}}(\mathbf{s})) = \chi(\eta_{\mathbf{e}}^{1/2} \rho_{\mathbf{s}} \eta_{\mathbf{e}}^{1/2}) = \chi(\zeta(p_{\mathbf{e}}^{1/2})\zeta(q_{\mathbf{s}})\zeta(p_{\mathbf{e}}^{1/2})) = \chi(\zeta(p_{\mathbf{e}}^{1/2} q_{\mathbf{s}} p_{\mathbf{e}}^{1/2})), \tag{17}$$

which, since $\chi \circ \zeta = \omega$, simplifies to

$$\chi(\psi_{\mathbf{e}}(\mathbf{s})) = \omega(p_{\mathbf{e}}^{1/2} q_{\mathbf{s}} p_{\mathbf{e}}^{1/2}). \tag{18}$$

Thus, in the Jordan algebra $\mathbb{S}_0$ the color measurement is expressed as a sandwich of split-quaternions with the same split-quaternion $p_{\mathbf{e}}^{1/2}$ on both sides. We must stress that this is different than the conjugation action $q \mapsto \alpha q \alpha^*$, in which, figuratively speaking, one of the bread slices appears as conjugated. The consequences of this particular sandwich formula will be explained in detail in the following section.

Given $\mathbf{e}$, it is of course useful to know how to obtain an explicit expression for $p_{\mathbf{e}}^{1/2}$. Let us recall, see [12], that every time-like split-quaternion $p = p_0 + p_1 i + p_2 j \in \mathbb{S}_0$ with a space-like vector part can be written as:

$$p = N(p)U(p) = N(p)(\cosh\vartheta + u_p \sinh\vartheta), \tag{19}$$

where $\cosh\vartheta = \frac{p_0}{N(p)}$ and $\sinh\vartheta = \frac{\sqrt{p_1^2 + p_2^2}}{N(p)}$, u_p being the following unit space-like split-quaternion:

$$u_p = \frac{p_1 i + p_2 j}{\sqrt{p_1^2 + p_2^2}}. \tag{20}$$

Using this polar form it is easy to check that such a split-quaternion p admits a unique square root, see [19], given by

$$p^{1/2} = \sqrt{N(p)}(\cosh(\vartheta/2) + u_p \sinh(\vartheta/2)). \tag{21}$$

In our case, since $p_{\mathbf{e}} = \zeta^{-1}(\eta_{\mathbf{e}}) = e_0 + e_1 i + e_2 j$, $p_{\mathbf{e}}^{1/2}$ can be easily calculated knowing the coordinates of $\mathbf{e}$, in fact:

$$\sqrt{N(p_{\mathbf{e}})} = \sqrt[4]{e_0^2 - e_1^2 - e_2^2}, \qquad \vartheta_{\mathbf{e}} = \operatorname{arctanh} ||\mathbf{v}_{\mathbf{e}}||, \qquad u_{p_{\mathbf{e}}} = \frac{e_1 i + e_2 j}{\sqrt{e_1^2 + e_2^2}}. \tag{22}$$

3.4 A sandwich without conjugate

In this paragraph we are going to provide an explanation of the lack of conjugation in the split-quaternion sandwich formula of eq. (18). To do so we start by recalling the geometric interpretation of the classic quaternion and split-quaternion conjugation formula used to obtain respectively classic rotations and Lorentz boosts.

It is well known that in classic quaternions the action of conjugation by a unit quaternion α, i.e. $q \mapsto \alpha q \alpha^*$ for any $q \in \mathbb{H}$, is an efficient way of encoding rotations of $\mathbb{R}^3$, [15]. Let us start by recalling that any rotation R in $\mathbb{R}^3$ is fully determined by a rotation angle ϑ and a rotation axis $v \in \mathbb{R}^3$. Moreover, when written with respect to the orthogonal splitting of $\mathbb{R}^3$ given by $v, v^\perp$, its matrix is

$$R = \begin{pmatrix} 1 & 0 \\ 0 & R_\vartheta \end{pmatrix}, \qquad \text{with} \quad R_\vartheta = \begin{pmatrix} \cos\vartheta & -\sin\vartheta \\ \sin\vartheta & \cos\vartheta \end{pmatrix}. \tag{23}$$

Let us now identify $\mathbb{H}$ with $\mathbb{R}^4$ as follows:

$$\begin{array}{rccc} \iota: & \mathbb{H} & \longrightarrow & \mathbb{R}^4 \\ & q_0 + q_1 i + q_2 j + q_3 k & \longmapsto & (q_0, q_1, q_2, q_3)^t. \end{array} \tag{24}$$

Any unit quaternion α can be written in the following form:

$$\alpha = \cos(\vartheta/2) + u\sin(\vartheta/2), \tag{25}$$

with u being a unit quaternion in $\mathrm{span}(i,j,k)$, [12]. We want to show that the conjugation action by α of a quaternion q, i.e. $q \mapsto \alpha q \alpha^*$, corresponds, to a rotation of axis $v = \iota(u)$ and angle ϑ in the three-dimensional vector subspace $V = \iota(\mathrm{span}(i,j,k))$ of $\mathbb{R}^4$.

Writing the elements of $\mathbb{H}$ w.r.t. the basis $1, u, u^\perp$, after straightforward computations, one can see that the left multiplication by α of a quaternion q in $\mathbb{R}^4$ corresponds to:

$$\iota(\alpha q) = \begin{pmatrix} R_{\vartheta/2} & O_2 \\ O_2 & R_{\vartheta/2} \end{pmatrix} \iota(q), \tag{26}$$

where O_2 refers to the 2×2 null matrix. Analogously, the right multiplication of q by its conjugate $\alpha^* = \alpha^{-1}$, gives:

$$\iota(q\alpha^*) = \begin{pmatrix} R_{-\vartheta/2} & O_2 \\ O_2 & R_{\vartheta/2} \end{pmatrix} \iota(q). \tag{27}$$

Combining eq. (26) and (27), one obtains the following matrix:

$$\iota(\alpha q \alpha^*) = \begin{pmatrix} Id_2 & O_2 \\ O_2 & R_{\vartheta} \end{pmatrix} \iota(q). \tag{28}$$

Comparing the latter expression with eq. (23) it is clear that $\iota(\alpha q \alpha^*)|_V = R\iota(q)$, hence we can conclude that the conjugation action corresponds to a rotation in V.

Let us consider now the case of split-quaternions and Lorentz boosts. Let us interpret $\mathbb{R}^3$ as the 3-dimensional Minkowski space-time and express it using the basis x, y, t, in which the first two elements are the spatial dimensions and the latter represents the temporal one. A Lorentz boost H in $\mathbb{R}^3$ is determined by an axis of fixed points $v \in \mathrm{span}(x,y)$ and an angle of hyperbolic rotation ϑ, called *boost rapidity*. Let us indicate with z the orthogonal vector to v in $\mathrm{span}(x,y)$, sometimes in the literature z is called *boost direction*. Expressing the boost matrix w.r.t. the basis v, z, t, one obtains the following analogue of eq. (23), with a hyperbolic rotation instead of a rotation:

$$H = \begin{pmatrix} 1 & 0 \\ 0 & H_\vartheta \end{pmatrix}, \qquad \text{with} \quad H_\vartheta = \begin{pmatrix} \cosh\vartheta & \sinh\vartheta \\ \sinh\vartheta & \cosh\vartheta \end{pmatrix}. \tag{29}$$

Notice that the hyperbolic rotation H_ϑ occurs on the vector subspace $\mathrm{span}(z,t)$ involving the boost direction and the time axis. Moreover $H_\vartheta^{-1} = H_{-\vartheta}$ and $H_{\vartheta_1} H_{\vartheta_2} = H_{\vartheta_1+\vartheta_2}$.

Now let us identify the split-quaternion algebra $\mathbb{S}$ with $\mathbb{R}^4$ via the function ι of eq. (24), $\iota : \mathbb{S} \longrightarrow \mathbb{R}^4$. As before, we define the vector subspace $V = \iota(\mathrm{span}(i,j,k))$. Our aim is to show that the conjugation action by α corresponds to a Lorentz boost in V. Notice that, in this identification, $\iota(k) = t$ plays the role of the time axis, while $\iota(\mathrm{span}(i,j)) = \mathrm{span}(x,y)$ represents the 2-dimensional space.

Let us consider a unit time-like split-quaternion α with space-like vector part. By eq. (19), α can be written as follows:

$$\alpha = \cosh(\vartheta/2) + u\sinh(\vartheta/2), \tag{30}$$

with $u = u_1 i + u_2 j$, being a unit split-quaternion. Let $w = -u_2 i + u_1 j$ be the vector orthogonal to u in $\mathrm{span}(i,j)$. As before, expressing the split-quaternions of $\mathbb{S}$ w.r.t. the basis $1, u, w, k$ and recalling the split-quaternion multiplication of eq. (9), we obtain that the left and right multiplication, respectively, of any $q \in \mathbb{S}$ by α in $\mathbb{R}^4$ are given by:

$$\iota(\alpha q) = \begin{pmatrix} H_{\vartheta/2} & O_2 \\ O_2 & H_{-\vartheta/2} \end{pmatrix} \iota(q), \qquad \iota(q\alpha) = \begin{pmatrix} H_{\vartheta/2} & O_2 \\ O_2 & H_{\vartheta/2} \end{pmatrix} \iota(q). \tag{31}$$

Since α is not a light-like split-quaternion, it admits a multiplicative inverse, and since we have supposed it to be a unit split quaternion, $\alpha^{-1} = \alpha^*$, see e.g. [12]. Thus the left multiplication by α^* is given by:

$$\iota(\alpha^* q) = \begin{pmatrix} H_{-\vartheta/2} & O_2 \\ O_2 & H_{\vartheta/2} \end{pmatrix} \iota(q). \tag{32}$$

Similarly to what was done in eq. (28), we can combine eqs. (31) and (32) obtaining:

$$\iota(\alpha^* q \alpha) = \begin{pmatrix} Id_2 & O_2 \\ O_2 & H_{\vartheta} \end{pmatrix} \iota(q). \tag{33}$$

Comparing the last equation with eq. (29) one can see that $\iota(\alpha^* q \alpha)|_V = H\iota(q)$, thus the conjugation action $q \mapsto \alpha^* q \alpha$ corresponds to a Lorentz boost in V of axis $\iota(u)$, direction $\iota(w)$ and rapidity ϑ. We must stress that the most commonly used formula (e.g. for the change of reference frames in relativity), is actually the inverse of the previous one, i.e. $q \mapsto \alpha q \alpha^*$ obtained changing the sign of the rapidity.

We have just seen how the conjugation action $\alpha \mapsto \alpha^* q \alpha$ corresponds to a boost in the vector subspace $V = \iota(\text{span}(i, j, k)) = \iota(\text{span}(u, w, k))$, in which the time coordinate is associated to the split-quaternion k via ι. However, as discussed in the previous paragraphs, we are interested in the sub-algebra $\mathbb{S}_0$ of split-quaternions having $q_3 = 0$ in which, recalling the isomorphism ω of eq. (14), time is associated to 1 instead of k.

It is convenient to introduce the vector subspace $W = \iota(\mathbb{S}_0) = \iota(\text{span}(1, i, j))$. For coherence with the relativistic interpretation of the model, we would like a split-quaternion sandwich formula corresponding to a Lorentz boost in W, instead of V.

Let us finally analyze the sandwich formula $q \mapsto \alpha q \alpha$, which is the one that will be used to implement the colorimetric transformations that will be discussed in the following section. Using the expressions in eq. (18) one obtains that this sandwich without conjugate, in $\mathbb{R}^4$, corresponds to:

$$\iota(\alpha q \alpha) = \begin{pmatrix} H_{\vartheta} & O_2 \\ O_2 & Id_2 \end{pmatrix} \iota(q), \tag{34}$$

where the matrix above is written w.r.t. the basis $\iota(1), \iota(u), \iota(w), \iota(k)$, hence it represents a boost in W of axis $\iota(w)$, direction $\iota(u)$ and rapidity ϑ.

Notice that this is different from the case of eq. (33), in which $\iota(u)$ was the boost axis and $\iota(w)$ its direction. Nevertheless, in both cases α is parameterized by u, thus we must stress that when using eq. (34) we pass as parameters, contained in α, the information associated to the boost direction and rapidity. This will be useful in the following section, since we associate the information of the illuminant vector to the boost direction and rapidity, that will be given directly as input parameters contained in α.

Note that $\iota(\alpha q \alpha)|_W$ corresponds to the matrix in eq. (7) after a suitable change of basis. Finally, let us recall that $p_{\mathbf{e}}^{1/2}$ in eq. (18) is not a unit split-quaternion, hence, to use eq. (34), one must identify $\alpha = U(p_{\mathbf{e}}^{1/2})$, and multiply eq. (34) by $N(p_{\mathbf{e}})$.

4 Application to white balance

In this section we use the color measurements modeled in the context of split-quaternions to implement a novel chromatic adaptation transform (CAT) for the automatic white balance (AWB) of digital images. AWB is a classic color processing meant to let the camera mimic the adaptation of the human visual system to the chromaticity of the illumination condition, often called illuminant. It consists of two steps: an illuminant estimation part, which identifies the illuminant(s) present in the visual scene, associating to them a 3-dimensional vector L, and a CAT, parametrized by L, returning an image representing how the scene would appear to an observer fully adapted to the illuminant. Several CATs have been proposed in the literature, see e.g. [1] for an overview, the

most widely used for applications is the von Kries CAT, see [22]. We propose a perceptual CAT, called *split-CAT* from now on, based on color measurements expressed using split-quaternions. A preliminary version of the algorithm, using simple Lorentz boosts, has been proposed in [14], a more complete version, using normalized Lorentz boosts, can be found in chap. 7 of [21]. We refer also the reader to [3], for a recent work using split-quaternions to perform Fourier analysis in the HSV color domain[2].

Let us start by representing the input image in the split-quaternion domain $\overline{\mathbb{S}_0^+}$. We consider an input image I with spatial domain denoted with $\mathcal{I}$, represented in the HCV color solid, thus $I(x) = (H(x), C(x), V(x))$, $\forall x \in \mathcal{I}$. To every pixel $x \in \mathcal{I}$, we associate the following split-quaternion $q(x)$ of $\overline{\mathbb{S}_0^+}$:

$$q(x) = V(x) + C(x)\cos(H(x))i + C(x)\sin(H(x))j. \tag{35}$$

Given the output L of an illuminant estimation algorithm, expressed in HCV color coordinates (H_L, C_L, V_L), we associate to it the effect $\mathbf{e} = (e_0, e_1, e_2) = (V_L, C_L \cos H_L, C_L \sin H_L)$. Then, the white balanced image q' represented in $\overline{\mathbb{S}_0^+}$ is obtained using the split-quaternion multiplication as follows:

$$q'(x) = p_{\mathbf{e}}^{-1/2} q(x) p_{\mathbf{e}}^{-1/2}, \quad \forall x \in \mathcal{I}, \tag{36}$$

in which $p_{\mathbf{e}}^{-1/2}$ is given by

$$p_{\mathbf{e}}^{-1/2} = \frac{1}{\sqrt{N(p_{\mathbf{e}})}}(\cosh(\vartheta_{\mathbf{e}}/2) - u_{p_{\mathbf{e}}}\sinh(\vartheta_{\mathbf{e}}/2)), \tag{37}$$

where $\sqrt{N(p_{\mathbf{e}})}$, $\vartheta_{\mathbf{e}}$ and $u_{p_{\mathbf{e}}}$ are calculated from $\mathbf{e}$ using eq. (22). Finally, we convert the image from $\overline{\mathbb{S}_0^+}$ back to the HCV color space. Some examples of outputs, obtained by processing images from the NUS Indoor Dataset [11], are depicted in Figure 1.

Figure 1: *Left*: input images. *Center*: output images after white balance using the von Kries CAT. *Right*: output images after white balance using the split-CAT. The white balanced images have been obtained using the same illuminant estimation. The illuminant vector is extracted automatically from the white patch of the color checker present in each image. The input images are taken from the open database [11].

The results of the von Kries CAT and those of the split-CAT look very similar at first glance. This is already quite remarkable, because it gives a first concrete proof of the fact that a transformation predicted *solely* by the rigorous mathematical interpretation of quantum measurement within the quantum information model of color perception leads to a color transformation that

[2]Note that this latter, unlike the HCV color space that will be used in the sequel, it is typically not considered a cone, but rather a cylinder.

produces results that are very similar to those of the most standard CAT. However, some hue shifts[3] can be seen in the output of the split-CAT, as shown by the hat in the third picture, first row, of Figure 1. In the following subsection we will stress that this is not an intrinsic feature of the split-CAT, but it depends on the choice of the HCV color space and we will propose how to reduce the hue shifts by modifying this color space.

4.1 Modification of HCV to encode Hering's opponency

The classic HCV color solid seemed to be a convenient approximation of the closed cone $\overline{\mathbb{S}_0^+}$ because of its conical shape. Nevertheless, HCV lacks of Hering's opponency, which instead is an intrinsic feature of the quantum information-based model of color perception. In fact, while blue and yellow are diametrically opposed in its hue configuration, it is not the case for red and green[4], as it can be seen in the first picture from the left of Figure 2. Moreover, we were noticing that red objects were slightly turning pinkish after applying the split-CAT in HCV. For these reasons, we propose two modified versions of the HCV color domain, denoted with H_1CV and H_2CV, obtained from HCV by modifying its H coordinate only. The objective is to modify the hue configuration on the circle in order to approximately recover the, non necessarily orthogonal, Hering's opponent axes. We must stress that a more general open issue in colorimetry is to understand which are the exact opponent unique hues and whether the opponent axes are orthogonal. Inter-observer variability and dependence on the viewing conditions clearly contribute to make the problem highly nontrivial.

The split-CAT implemented in H_1CV or H_2CV gives overall better qualitative and quantitative, as we will see in the next paragraph, results. Figure 3 shows an example[5] obtained processing images from [11].

Let us explain a bit more in detail how the color solids H_1CV and H_2CV have been constructed. We modified the H coordinate trying several functions, obtained using simple interpolation techniques in 1-dimension and selected the two best performing ones on the images in the rendering of the red hue, let us call them f_1, f_2. Both $f_1, f_2 : [0, 2\pi] \to [0, 2\pi]$ are 2π-periodic and invertible[6]. The coordinates H_i are obtained from H by $\mathrm{H}_i = f_i^{-1}(\mathrm{H})$, $i = 1, 2$. In particular:

1. f_1 is obtained requiring the red to stay fixed, and the green to be diametrically opposed to the red, hence it is obtained by quadratic interpolation of the points $(0, 0)$, $(2\pi/3, \pi)$, $(2\pi, 2\pi)$. It can be explicitly written as a parabola $f_1(x) = \frac{1}{4}\left(7x - \frac{3}{2\pi}x^2\right)$. As depicted in Figure 2 (*Center*), red and green are now opponent, but the blue is diametrically opposed to an orangish yellow. Furthermore these opponent axes are not orthogonal, but separated by an angle of 30°.

2. f_2 is obtained by fixing again the red and moving the green to be diametrically opposed to it, then moving the yellow and the blue in order to have an angle of 60° between the two opponent axes, as in Figure 2 (*Right*). f_2 was obtained via quadratic piece-wise interpolation of the points $(0, 0)$, $(\pi/3, 2\pi/3)$, $(2\pi/3, \pi)$, $(4\pi/3, 5\pi/3)$, $(2\pi, 2\pi)$.

These simple interpolation techniques enabled us to define two color solid that incorporate, better than HCV, Hering's opponent mechanism. Clearly the fine-tuning procedure detailed in footnote 6

[3]The most visible case is the one of red objects shifting towards magenta.

[4]Note that by yellow, blue, red and green here we mean the representations in the HCV color solid of the RGB vectors $(255, 255, 0)$, $(0, 0, 255)$, $(255, 0, 0)$, $(0, 255, 0)$. As remarked before there is no exact, nor clear, correspondence between these vectors and Hering's opponent hues, or unique hues.

[5]Notice that in particular does not produce a magenta shift of red objects, see e.g. the white-red box with a flower depicted on it.

[6]Two options for the opponent axes were considered: red-green, yellow-blue and red-green, orange-blue, see also footnote 4. Let us call them $\mathrm{a_Y}$ and $\mathrm{a_O}$, respectively. The adopted interpolation techniques were linear and quadratic (piece-wise), let us denote them with l and q, respectively. Higher order interpolations (with polynomials of degrees 3 and 4) were tested as well, but there was no visible difference w.r.t. the quadratic case, hence they were not considered. Finally, 5 different angles between the opponent axes were taken into account: 30°, 60°, 90°, 120°, 150°, for a total of 20 possible functions. The best performing ones, f_1 and f_2 correspond to the choices $(\mathrm{a_O}, q, 60°)$ and $(\mathrm{a_Y}, q, 120°)$ for the parameters defined above.

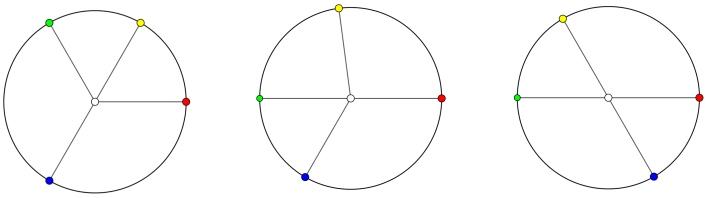

Figure 2: Red, yellow, green and blue hue positions in the hue-chroma planes of the HCV, H_1CV and H_2CV color spaces. The images have been generated by the authors for the purposes of the present paper.

Figure 3: *Left*: output of the split-CAT in HCV. *Center*: output of the split-CAT in H_1CV. *Right*: output of the split-CAT in H_2CV. These are there output pictures of an original image taken from the open database [11].

could be iterated and improved. However, the meaningful information to stress out is the fact that going in the direction of better integrating Hering's opponent mechanism in a color solid provides better results and it constitutes an appropriate context in which testing future applications of the theoretical model summarized in section II, see section V for future research directions on this topic.

4.2 Quantitative evaluation of the color checker rendering

We evaluated four CATs: the von Kries CAT, the split-CAT implemented in HCV, H_1CV and H_2CV.

We started by generating linear PNG images applying linear demosaicing on the RAW RGB images provided with the NUS Indoor dataset (Canon 1Ds Mark III, 105 images), [11]. We automatically detected the color checker present in each image and extracted the nineteenth patch (the white one) as ground truth illuminant vector. Using the extracted ground truths we corrected the mentioned PNG images using the four different CATs.

Clipping cases were managed by dividing the image by its maximum. Then we detected all the color checkers (a RGB vector corresponding to each patch) in the output images, still using the automatic color checker detection functions.

For each CAT we considered the set of detected color checkers and calculated the distance between each of them and the standard benchmark color checker, enlightened by the D65 illuminant. As distance we used seven state-of-the art color metrics listed in table 1. This distance was obtained by calculating, for each patch, its distance from the corresponding one in the benchmark color checker and then averaging over the 24 patches. For each CAT we averaged the distances of the color checkers over the 105 images of the dataset, obtaining the values reported by table 1. Both the algorithm for the automatic detection of the color checker and the different color metrics were used as implemented in the open-source Python package *Colour*[7].

Lower values in this table mean that the color checker rendering of a certain CAT is closer to the benchmark color checker. We can see that H_1CV is better performing than H_2CV. Furthermore,

[7]See https://colour.readthedocs.io/en/develop/.

Metrics	von Kries	split HCV	split H_1CV	split H_2CV
CIE 1994	25.66	25.01	24.86	**24.85**
DIN99	26.25	25.48	**25.28**	25.39
CIEDE 2000	22.53	**22.10**	22.44	22.41
CAM02 UCS	25.99	**25.31**	**25.31**	25.34
CAM02 LCD	33.87	32.99	**32.84**	32.93
CAM16 UCS	26.01	**25.28**	25.31	25.35
CAM16 LCD	33.87	32.99	**32.84**	32.94

Table 1: Comparison between the von Kries CAT and split-CAT implemented in different HCV spaces.

according to this evaluation, it is slightly better to use the implementation in H_1CV than in HCV. The value in bold highlights the smallest among the four values in the line in which it belongs, it can be seen that the three split-CATs perform better than the von Kries CAT w.r.t. this criterion.

5 Conclusions and future perspectives

In this paper we have proposed and tested the first concrete application of a recently developed quantum-like framework for color perception. This application consists at defining a theoretically-based chromatic adaptation transform, the split-CAT, to perform the classic color processing task of automatic white balance. To do so, we started by enriching the algebraic structure of the quantum-like model by providing an alternative, isomorphic representation of the Jordan algebra $\mathcal{A}$, i.e. the sub-algebra $\mathbb{S}_0$ of the split-quaternion algebra $\mathbb{S}$, with $\overline{\mathbb{S}_0^+}$ as domain of positivity.

In terms of split-quaternions, the fundamental measurement equation, eq. (3), used in [9, 7] to define a perceived color as the outcome of a measurement procedure, is expressed by a so-called sandwich formula, see eq. (18). This sandwich formula is different from the one usually used classically, since none of the terms appears conjugated. We better clarified this peculiarity by writing explicitly the action of the sandwich formula in $\mathbb{R}^4$.

Finally, we defined the split-CAT as the action of a sandwich, parametrized by the effect associated to the illuminant. To do so, we associated the pixels of a digital image represented in the HCV color solid to elements of $\overline{\mathbb{S}_0^+}$.

Qualitative considerations about the color rendering of the output images led to the definitions of two modified versions of the HCV color solid, H_1CV and H_2CV, obtained via simple interpolation techniques meant to modify the hue configuration, making it approximately closer to having Hering-like opponent axes. Then, we provided a quantitative evaluation of the performance of the classic von Kries CAT, the split-CAT in HCV, H_1CV and H_2CV in the overall rendering of the color checker patches. The results show that H_1CV provides the best score.

Further evaluations of the performance of the proposed algorithm are clearly possible, e.g. one could perform systematic comparisons with other state-of-the art CATs, using as a reference the corresponding colors datasets, as in [1].

An important open question concerns the domain for the implementation. A possible approach is to continue fine-tuning the HCV color domain, or use other existing color spaces, like CIELab or IPT, keeping in mind that the algorithm is designed to preserve a conic shaped solid, hence color solids having more irregular shapes will probably produce artifacts that should be treated separately.

A different, interesting, perspective concerns the idea of studying alternative ways of integrating Hering's opponent mechanism in a color solid, which are more related to psychophysical data, see e.g. [16, 17], rather than performing a purely engineering-oriented a posteriori manipulation of existing color solids.

Acknowledgments

This work has been partially carried out with the financial support of Huawei Technologies France SASU and the European Research Council Advanced Grant (ERC AdG, ILLUSIVE: Foundations of Perception Engineering, 101020977).

References

[1] CIE 160-2004, A review of chromatic adaptation transforms. ISBN:9783901906305, 2004.

[2] John C Baez. Division algebras and quantum theory. *Foundations of Physics*, 42(7):819–855, 2012.

[3] E. Bayro-Corrachano, Z. Vazquez-Flores, and U. Uriostegui-Legorreta. The Lorentz Group Using Conformal Geometric Algebra and Split Quaternions for Color Image Processing: Theory and Practice. *IEEE Access*, 11:56785–56800, 2023.

[4] M. Berthier. Geometry of color perception. Part 2: perceived colors from real quantum states and Hering's rebit. *The Journal of Mathematical Neuroscience*, 10(1):1–25, 2020.

[5] M. Berthier, V. Garcin, N. Prencipe, and E. Provenzi. The relativity of color perception. *Journal of Mathematical Psychology*, 103:102562, 2021.

[6] M. Berthier and E. Provenzi. From Riemannian trichromacy to quantum color opponency via hyperbolicity. *Journal of Mathematical Imaging and Vision*, 63(6):681–688, 2021.

[7] Michel Berthier, Nicoletta Prencipe, and Edoardo Provenzi. A quantum information-based refoundation of color perception concepts. *SIAM Journal on Imaging Sciences*, 15(4):1944–1976, 2022.

[8] Michel Berthier and Edoardo Provenzi. The quantum nature of color perception: Uncertainty relations for chromatic opposition. *Journal of Imaging*, 7(40), 2021.

[9] Michel Berthier and Edoardo Provenzi. Quantum measurement and colour perception: theory and applications. *Proceedings of the Royal Society A*, 478(2258):20210508, 2022.

[10] Paul Busch, Marian Grabowski, and Pekka J Lahti. *Operational quantum physics*, volume 31. Springer Science & Business Media, 1997.

[11] D. Cheng, B. Price, S. Cohen, and M.S. Brown. Beyond white: Ground truth colors for color constancy correction. In *Proceedings of the IEEE International Conference on Computer Vision*, pages 298–306, 2015.

[12] M. Gogberashvili. Split quaternions and particles in (2+1)-space. *The European Physical Journal C*, 74(12):1–9, 2014.

[13] M. Gogberashvili. (2 + 1)-Maxwell equations in split quaternions. *Physics*, 4(1):329–363, 2022.

[14] A. Guennec, N. Prencipe, and E. Provenzi. Color correction with lorentz boosts. In *2021 The 4th International Conference on Image and Graphics Processing*, ICIGP 2021, page 162–168, New York, NY, USA, 2021. Association for Computing Machinery.

[15] A. J. Hanson. *Visualizing Quaternions*. Series in Interactive 3D Technology, Morgan Kaufmann Publishers, 2006.

[16] L.M. Hurvich and D. Jameson. Some quantitative aspects of an opponent-colors theory. II. brightness, saturation, and hue in normal and dichromatic vision. *JOSA*, 45(8):602–616, 1955.

[17] L.M. Hurvich and D. Jameson. Some quantitative aspects of an opponent-colors theory. III. changes in brightness, saturation, and hue with chromatic adaptation. *JOSA*, 46(6):405–415, 1956.

[18] M Özdemir and Abdullah A Ergin. Rotations with unit timelike quaternions in minkowski 3-space. *Journal of geometry and physics*, 56(2):322–336, 2006.

[19] Mustafa Özdemir. The roots of a split quaternion. *Applied Mathematics Letters*, 22(2):258–263, 2009.

[20] M. M. Postnikov. *Lie groups and Lie algebras*. MIR Publishers, 1986.

[21] Nicoletta Prencipe. *Theory and applications of a novel formulation of the space of perceived colors*. PhD thesis, Université de Bordeaux, 2022.

[22] J. von Kries. Chromatic adaptation. *Festschrift der Albrecht-Ludwigs-Universität*, pages 145–158, 1902.